Interaction of lithium with graphene: An *ab initio* study

M. Khantha,[1] N. A. Cordero,[2] L. M. Molina,[3] J. A. Alonso,[4] and L. A. Girifalco[1]
[1]*Department of Materials Science and Engineering, University of Pennsylvania, Philadelphia, Pennsylvania 19104, USA*
[2]*Departamento de Fisica, Universidad de Burgos, E-09001 Burgos, Spain*
[3]*Aarhus University, Interdisciplinary Nanoscience Center, DK-8000 Aarhus C, Denmark*
[4]*Departamento de Fisica Teorica, Universidad de Valladolid, E-47011 Valladolid, Spain*
(Received 6 February 2004; revised manuscript received 24 June 2004; published 24 September 2004)

The interaction potential of a Li atom with a graphene layer is calculated using the local density approximation to the density functional theory. Two configurations corresponding to different separations between Li in neighboring supercells were considered to determine the effect of Li-Li interaction on the binding of Li to graphene. The equilibrium position of Li is not affected by the Li-Li interaction and remains the same in both cases. It is equal to 3.1 a.u. above graphene with the Li at the center of a hexagonal ring formed by the carbon atoms. However, the binding energies differ substantially in the two configurations. The binding energy of Li is 0.934 eV in configuration A when the Li-Li separation in adjacent supercells is 9.22 a.u. The binding energy is 1.598 eV in configuration B corresponding to a separation 18.45 a.u. between adjacent Li atoms. There is substantial charge transfer from both lithium and carbon atoms (including those that do not surround the lithium) to a region between the Li and graphene at the minimum energy configuration. The interaction potential for both configurations can be fitted to a sum of a screened Yukawa potential and a linear superposition of power-law functions of type r^{-n}, where n is an integer. The density functional theory underestimates the attractive contribution of dispersion forces for large separations. The attractive interaction potential calculated for Li positions much greater than the equilibrium distance from graphene may therefore need to be corrected.

DOI: 10.1103/PhysRevB.70.125422 PACS number(s): 71.20.Tx, 68.35.−p, 71.15.Mb

I. INTRODUCTION

The first synthesis of lithium metal intercalated into graphite resulting in a graphite intercalation compound (GIC) was made in 1955 by Herold.[1] Extensive research has been carried out since then on Li-GIC's (LiC_6) to investigate charge transfer and staging structure which is of interest for the development of rechargeable Li-ion batteries.[2–6] Carbon nanotubes consist of one or more concentric rolled up planes of graphite.[7,8] Currently, many theoretical[9–16] and experimental[17–22] studies have focused attention on lithium intercalated carbon nanotubes because these offer much higher Li capacity ranging from $Li_{1.6}C_6$ to $Li_{2.7}C_6$ (Refs. 20 and 22–24) depending on processing conditions. Additionally, the doping of single wall carbon nanotubes (SWCNT's) by Li and K is known to enhance conductivity and hydrogen storage capacity.[25]

Both scientific and technological progress requires a systematic understanding of interactions in Li-graphitic systems. The potential energy curves for the interaction of Li with graphitic systems and the nature of electron transfer in these structures are of particular interest. In this paper, we consider the simplest system, Li atoms interacting with a single layer of graphite (graphene layer). The van der Waals interactions in the graphitic systems are unique in that the potential energy of interaction between graphene sheets and between nanotubes can be described by a single universal graphitic potential.[26] Both the Li-graphene and Li-nanotube systems are characterized by a combination of ionic and van der Waals forces. We present the charge distribution and the potential energy of interaction in the Li-graphene system using density functional theory in this paper. The interactions in the Li-nanotube system using the same methodology will be discussed separately elsewhere.

Many types of electronic structure calculation schemes have been used to elucidate charge transfer and the interaction of Li atoms in GIC's (Refs. 27–31) and SWCNT's.[9–16,32] In contrast, we are aware of only one study[9] of the Li-graphene system. The binding energy of Li onto a graphene layer was found to be 1.70 eV at an equilibrium distance of 3.97 a.u.. from the graphene plane[9] (the adsorption site was at the top of the hexagon's center) based on a semiempirical Hartree-Fock linear combination of atomic orbitals scheme. The electron transfer from Li to graphene was 0.72 electrons. The interaction potential of Li as a function of its separation from graphene was not calculated in that work. The adsorption energy of Li on graphene may be compared with the intercalation energy per carbon atom of Li in graphite which saturates around 1.4 eV for a composition of $Li_{0.35}C$.[16]

II. LITHIUM-GRAPHENE INTERACTION

We use the density functional theory (DFT) to determine the interaction between a Li atom and a graphene sheet. The calculations were done using the FHI98MD code developed by Scheffler *et al.*[33] This code uses supercell geometry and the electronic wave functions are expanded in a basis of plane waves. The electrons explicitly included in the calculation are the $(2s^2 2p^2)$ electrons of carbon and the $(2s^1)$ electron of lithium. The core electrons $(1s^2)$ of carbon and lithium are replaced by pseudopotentials.[34] Nonlocal, norm-conserving

TABLE I. Structural properties of bulk lithium and comparison with other calculations and experiments.

Lithium	Structure	Cohesive energy (mRy)	a_0 (a.u.)	B (kbar)
Present calculation	hcp*	136.78	5.64(c/a=1.633)	149.7
	fcc	136.07	8.03	148.2
	bcc	135.06	6.35	148.18
Cho *et al.*[a]	hcp*	137.01	5.71(c/a=1.630)	152
	fcc	136.99	8.09	151
	bcc	136.45	6.34	153
Staikov *et al.*[b]	hcp		5.83(c/a=1.633)	133
	fcc*		8.20	134
	bcc		6.51	135
Dacorogna and Cohen[c]	hcp*		5.71(c/a=1.630)	137
	fcc		8.09	138
	bcc		6.43	130
Experiment[d]	hcp	124.5	5.88(c/a=1.637)	126.5
Experiment[e]	bcc		6.60	116

[a]Reference 40.
[b]Reference 41.
[c]Reference 39.
[d]Reference 42.
[e]Reference 43.

pseudopotentials of the Troullier-Martins form[35] were used for both carbon and lithium in the Kleinman-Bylander separable form.[36] The nonlocality in the pseudopotential was restricted to $l=2$ while the s component was treated as a local part of the pseudopotential. The local density approximation (LDA) as parametrized by Perdew and Wang[37] was used for exchange and correlation.

The carbon pseudopotential was tested for pure graphite. The in-plane C-C bond length was to be 2.66 a.u. and the separation between planar graphitic layers was 6.27 a.u. The corresponding experimental values[7] are 2.68 and 6.34 a.u., respectively. The C-C bond length for a single graphene layer was fixed to be 2.66 a.u. (the same as for graphite). The Li pseudopotential includes an additional nonlinear treatment of the exchange-correlation interaction between core and valence electrons. The pseudopotential energy without this correction treats this interaction as linearly dependent on the valence electron density. The nonlinear correction[33,34] is usually needed to describe the alkali metals. This correction is implemented by adding a partial core density to the valence density in the unscreening of the pseudopotential. The partial core density reproduces the full core density outside a chosen cutoff radius (a value of 1.6 a.u. was used for Li) while it gives a smoother function within this radius.

The pseudopotential for lithium was tested by calculating the structural stability of lithium in hcp, fcc, and bcc phases and comparing the results with previous studies. Although lithium is the simplest metal, it is well known that its phase structure is quite difficult to reproduce from *ab initio* calculations.[38–41] Some calculations[38,41] predict the fcc phase to be the lowest energy structure while experiments[42,43] and other calculations[39,40] predict the hcp phase to be the lowest in energy. The difficulty lies in the small energy difference between the hcp and fcc phases. Both Hamann[44] and Troullier-Martins type[35] pseudopotentials have been employed with and without the nonlinear core-valence correction in previous calculations.[39,40]

We used a plane-wave basis set with an energy cutoff of 40 Ry and minimized the total energy with respect to the interatomic distance for each structure. The number of special k points in the irreducible Brillouin zone was 50 for hcp, 10 for fcc, and 8 for bcc phase. The convergence criterion was such that all energies were converged to 2.7 meV. The equilibrium lattice parameter, cohesive energy, and the bulk modulus obtained for the lowest energy configuration for different structures are listed in Table I. These were calculated by fitting to Murnaghan's equation of state.[45] We also list results from other theoretical calculations and experiments in Table I for comparison. The lowest energy phase is indicated by an asterisk. We find the hcp phase to be the lowest energy and the ordering of the phases is $E_{\mathrm{hcp}}<E_{\mathrm{fcc}}<E_{\mathrm{bcc}}$. The equilibrium properties of all the phases are in agreement with results of Cho *et al.*[40] and differ 5–10% from experiments in the range expected from density functional calculations using local density approximation.

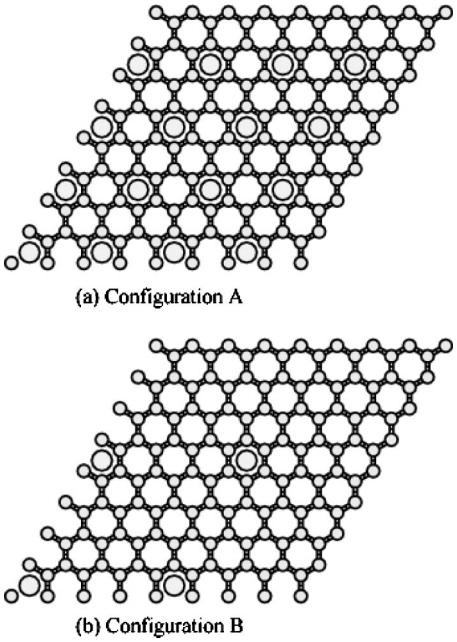

FIG. 1. The arrangement of Li atoms above the graphene plane. The Li (big circles) are positioned at the center of a hexagonal ring formed by carbon atoms (small circles). (a) Configuration A where the separation between adjacent Li atoms is 9.22 a.u. (b) Configuration B where the separation between adjacent Li atoms is 18.45 a.u.

Two different configurations of the Li-graphene system shown in Figs. 1(a) and 1(b) and referred henceforth as A and B were used in the DFT calculations. These configurations were chosen to determine the effect of interaction between closely spaced Li atoms on the binding of Li to graphene. The hexagonal unit cell of the Li-graphene system in Fig. 1(a) (configuration A) contains eight carbon atoms and one lithium atom. The separation between neighboring Li atoms is 9.22 a.u. in Fig. 1(a). The hexagonal unit cell in Fig. 1(b) (configuration B) contains 32 carbon atoms and 1 Li atom. The linear dimension of the supercell is twice as big as in Fig. 1(a) and the separation between adjacent Li equals 18.45 a.u. It is necessary to ensure that the z axis of the periodic supercell (perpendicular to the graphene layer) is large enough that there is no interaction between graphene sheets belonging to adjacent supercells.[46] This is required to study the binding of Li to an isolated graphene sheet. A distance of 20 a.u. along the z axis was found to be sufficient to ensure energy convergence for both configurations shown in Fig. 1. This is in conformity with earlier studies[46] on the adsorption of H_2 on graphene layers.

A plane-wave basis set with an energy cutoff of 50 Ry was used. The integration over the Brillouin zone was done using the Monkhorst-Pack scheme.[33] The number of k points for configuration A was 20 while that for configuration B was 8. The convergence criterion was such that all energies were converged to 2.7 meV. The energy of the configuration when Li is on top of a carbon atom is always much higher than the energy when the Li is at the center of the hexagon formed by carbon atoms. We therefore present results only for the case when Li is at the center of the hexagon. A series

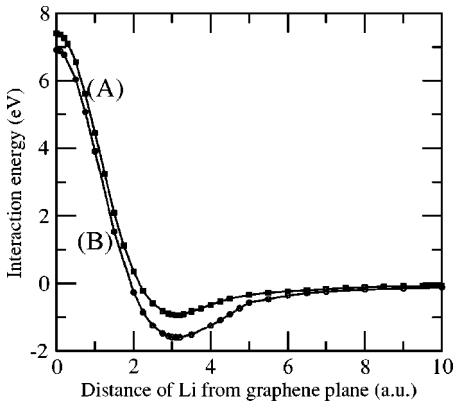

FIG. 2. The interaction energy of Li with graphene in configuration A (curve labeled A) and in configuration B (curve labeled B).

of static calculations was performed to determine the interaction potential of Li with graphene. The Li atoms were kept fixed at different distances along a line perpendicular to the graphene layer through the center of a hexagon of carbon atoms. The energy was minimized by relaxing the electronic degrees of freedom. The interaction energy at a fixed Li distance was obtained by subtracting the energy of the graphene plane and the isolated Li atom from the energy of the Li-graphene configuration.

The interaction potential is shown in Fig. 2 for configurations A and B. The binding energy ($|$minimum interaction energy$|$) for configuration A is 0.934 eV when the Li atom is 3.1 a.u. (1.64 Å) from the graphene plane above the center of a hexagon of carbon atoms. The binding energy for configuration B, 1.598 eV, is higher than in configuration A. However, the equilibrium position of Li above graphene (3.1 a.u.) is the same for configuration B as for configuration A. The energy when the Li is located on the graphene plane is 7.40 eV in configuration A and 6.91 eV in configuration B. An earlier study of the same problem by some of the authors[47] using Hamann-type pseudopotentials for Li and C with linear core-valence exchange correlation gave the erroneous result that the energy of the Li on the graphene plane was lower than the energy of Li at very large separations. As the distance of the Li atom reaches its asymptotic value of 10 a.u. (which is the largest separation allowed for a superlattice of size 20 a.u. in the direction perpendicular to the graphene plane), the interaction energy is $\sim$0.1 eV in both configurations.

It is clear from Fig. 2 that the interaction between Li (configuration A) has a significant effect on the binding energy of Li to graphene. A comparison of curves A and B in Fig. 2 shows that the Li-Li interaction between Li separated by 9.22 a.u. (configuration A) is repulsive and persists even when the Li ions are 10 a.u. from graphene. The repulsive interaction originates due to the charge transfer that takes place between Li and graphene leaving a positively charged cation at the original location of the Li atom. The charge transfer remains significant even when Li is 10 a.u. from graphene. The Li-graphene interaction remains nonzero at this distance because the screening of Coulomb interaction between negatively charged regions close to the graphene layer due to the presence of cations is not adequate when Li

is far away from graphene. The long-ranged Coulomb interaction between the cations does not vanish even when the distance between cations is 18.45 a.u. However, at the equilibrium position, the screening is almost total in both configurations irrespective of the strength of Li-Li interactions. These and other features of the interaction potential can be better understood by examining the charge distribution and charge transfer in the two configurations. This is discussed in the next section.

III. CHARGE REDISTRIBUTION, CHARGE TRANSFER, AND INTERACTION POTENTIAL

Let $\rho_{tot}(\mathbf{r})$ represent the calculated charge density for the total system (Li and graphene), $\rho_g(\mathbf{r})$ the charge density of a graphene layer (without Li), and $\rho_{\mathrm{Li}}(\mathbf{r})$ the charge density of an isolated Li atom located at the same position as in the total system. The charge density difference is defined by the relation

$$\rho_{\mathrm{diff}}(\mathbf{r}) = \rho_{\mathrm{tot}}(\mathbf{r}) - [\rho_{\mathrm{g}}(\mathbf{r}) + \rho_{\mathrm{Li}}(\mathbf{r})]. \quad (1)$$

Figures 3(a) and 3(b) show the total charge density of the Li and graphene system in configurations A and B, respectively, when the Li is located 3.1 a.u. above graphene (the minimum energy position). The charge density is shown on a plane 3.1 a.u. above the graphene layer [parallel to the *xy* plane in Figs. 1(a) and 1(b)] and containing the Li atom. The charge density of pure graphene on a plane 3.1 a.u. above the layer is comparable to that due to only lithium atoms located at $z=3.1$ a.u. The charge density distribution in Figs. 3(a) and 3(b) reflects the triangular network of Li located at the centers of hexagonal rings of carbon atoms. There is little difference in the maximum charge density observed inside the hexagonal rings containing Li and surrounded by C in configurations A and B. However, the charge density in and around carbon rings not containing Li differ in Figs. 3(a) and 3(b). There is considerable overlap of charge density due to interaction between Li separated by 9.22 a.u. in Fig. 3(a) resulting in higher charge density and distorted elliptical profile over hexagonal rings not containing Li. There is minimal interaction between Li ions separated by 18.45 a.u. in configuration B as seen from the charge density profile in Fig. 3(b).

It is useful to compare the difference of charge density $\rho_{\mathrm{diff}}(\mathbf{r})$ defined in Eq. (1) in configurations A and B for different positions of Li from the graphene plane. We choose the following values to compare the effect of interactions between Li ions on charge screening and transfer: (a) 3.1 a.u. (equilibrium position), (b) 2.0 a.u., and (c) 4.0 a.u. The difference of charge density is shown on a plane perpendicular to the graphene layer (*yz* plane) and containing the Li atom. In this series of plots shown in Figs. 4–6, a carbon atom is located at the origin and at positions along the horizontal axis denoted by label C. The labels *X* and *M* refer to the center of a hexagon and the midpoint between two closest carbon atoms, respectively. The vertical axis denotes positions perpendicular to the graphene layer.

Figures 4(a) and 4(b) show the difference of charge density corresponding to configurations A and B, respectively,

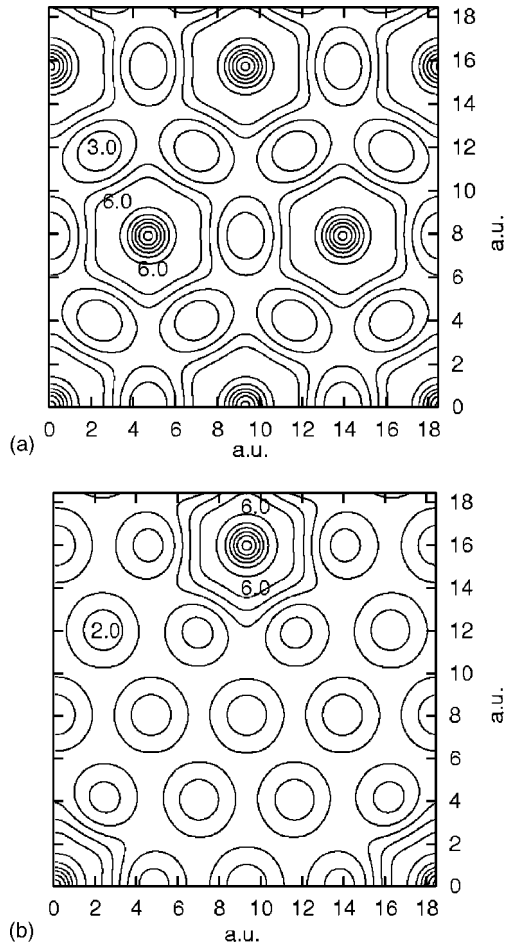

FIG. 3. Contours of constant electron density $\rho_{\mathrm{tot}}(\mathbf{r})$ of Li graphene on a plane 3.1 a.u. above the plane of the carbon nuclei in configurations A (a) and B (b). The units for the electron density are $1.0\times10^{-3}e/(\mathrm{a.u.})^3$. The contours are equally spaced with an interval $1.0\times10^{-3}e/(\mathrm{a.u.})^3$.

when Li is 3.1 a.u. above graphene. The single Li atom in the supercell is located at (2.66, 3.1) a.u. Positive values indicate net gain of electronic charge and vice versa. There is net gain of electronic charge in the region between Li and graphene while there is net loss of electronic charge just above the graphene layer and above the Li. The net gain of charge is due to charge transfer from both the Li and the carbon atoms surrounding the Li. This is evident from the net loss of charge density close to the graphene layer around the immediate carbon atoms surrounding the Li. The charge redistribution in the region of the hexagonal ring surrounding the Li is similar in appearance and magnitude in both configurations. The equilibrium position of Li above graphene is largely determined by the charge redistribution that takes place in this region. Consequently, it is the same for both configurations. The binding energy of Li is, however, determined by the screening and the balance between attractive and repulsive interactions. The charge redistribution around all carbon and lithium positions determines this value. There are notable differences in the charge redistribution just above and below the position of Li in the two cases. The Coulomb repulsion is enhanced in configuration A due to the proximity

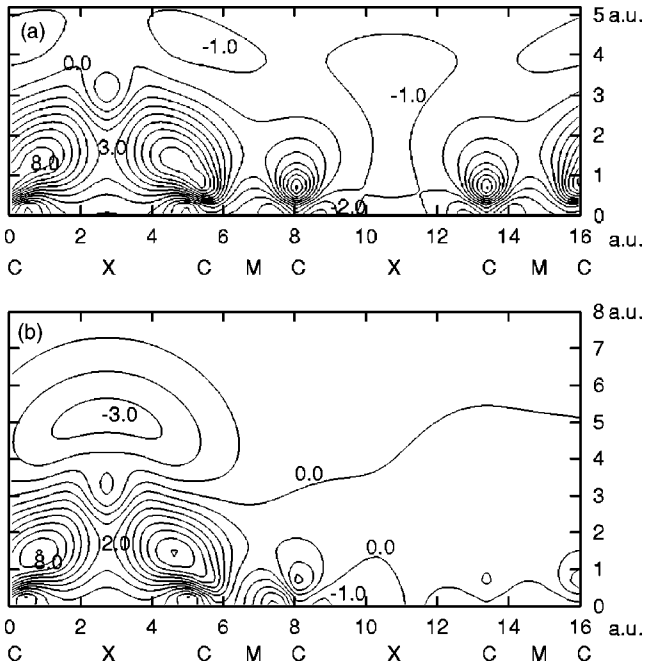

FIG. 4. The difference in charge density $\rho_{\mathrm{diff}}(\mathbf{r})$ on a plane perpendicular to graphene and containing the Li atom for configurations A (a) and B (b). The Li is at its equilibrium position 3.1 a.u. above the graphene layer at the center of a hexagonal ring of carbon. Its coordinates are (2.66, 3.1) a.u. The units of the electron density are $1.0\times10^{-3}e/(\mathrm{a.u.})^3$. The contours are equally spaced with an interval $1.0\times10^{-3}e/(\mathrm{a.u.})^3$. The contours closest to the graphene layer correspond to negative values and indicate net loss of electron density.

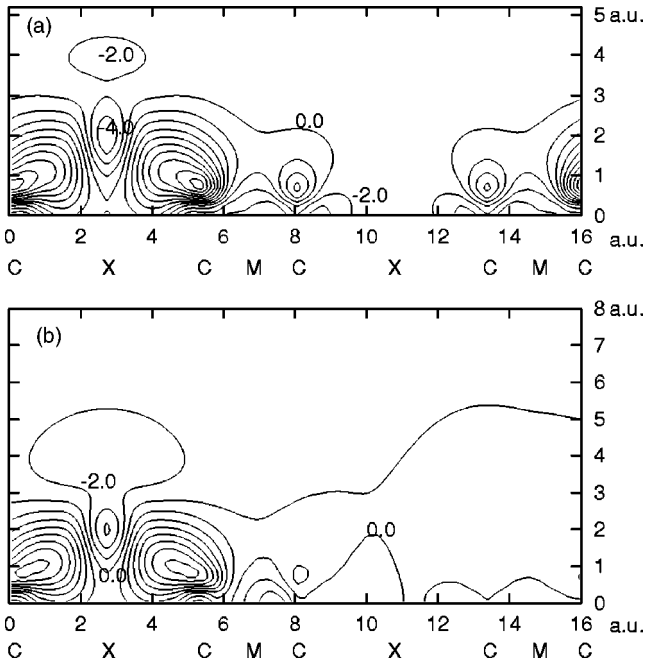

FIG. 5. The difference in charge density $\rho_{\mathrm{diff}}(\mathbf{r})$ on a plane perpendicular to graphene and containing the Li atom for configurations A (a) and B (b). The Li is positioned 2.0 a.u. above the graphene layer and its coordinates are (2.66, 2.0) a.u. The units of the electron density are $1.0\times10^{-3}e/(\mathrm{a.u.})^3$. The contours are equally spaced with an interval $2.0\times10^{-3}e/(\mathrm{a.u.})^3$. The contours corresponding to the maximum gain of electron density [near coordinates (0.0, 0.8) a.u. and (5.2, 0.8) a.u.] have the value $18.0\times10^{-3}e/(\mathrm{a.u.})^3$ in configuration A and $14.0\times10^{-3}e/(\mathrm{a.u.})^3$ in configuration B. Contours closest to the graphene layer correspond to negative values and indicate net loss of electron density.

of regions of similar charge arising from closely spaced Li ions. This is responsible for the lower binding of configuration A compared to that of configuration B.

Figures 5(a) and 5(b) show the difference of charge density corresponding to configurations A and B, respectively, when Li is 2.0 a.u. above graphene. There is more charge transfer in the region between graphene and lithium when Li ions interact (configuration A) compared to when the Li ions are well separated. However, the charge transfer around the position of the Li cation is greater in B than in A. The reduced Coulomb repulsion makes the interaction energy of configuration B lower than A. Compared to Figs. 4(a) and 4(b), there is less charge transfer from the carbon positions surrounding the Li just above the graphene, giving rise to less binding at 2 a.u. compared to 3.1 a.u.

Figures 6(a) and 6(b) show the difference of charge density corresponding to configurations A and B, respectively, when Li is 4.0 a.u. above graphene. The charge redistribution (corresponding to net loss of charge density) just above the graphene plane around carbon surrounding the Li is similar in the two configurations as in Fig. 4. There is more charge transfer from Li position to the region between Li and graphene in configuration B than in A. The consequent increase in Coulomb repulsion is, however, offset by the screening due to greater degree of charge redistribution above the position of Li compared to that in configuration A. These factors lead to the enhanced binding (lower interaction energy) at this position of Li in configuration B compared to that in configuration A.

The substantial charge transfer and redistribution that occurs for all positions of Li suggests the formation of dipoles in the Li-graphene system. This implies surface dipole corrections to the total energy calculations based on supercell geometry.[33] The results presented above did not employ the dipole correction. We have repeated the same calculations including the surface dipole correction[33] for several positions of Li both smaller and larger than the equilibrium distance (3.1 a.u.) in configuration A. The maximum correction to the energy occurs when Li is positioned closer than the equilibrium distance from graphene. The correction to the interaction potential is $\sim$0.03 eV when Li is 2.0 a.u. from graphene and less than 0.01 eV when Li is 3.1 a.u. from graphene. There is no detectable difference in the charge density difference when Li is greater than 2.5 a.u. from graphene. When Li is 2.0 a.u. away from graphene, the difference of charge density calculated with surface dipole correction does not have the lobe of net charge density loss seen at (2.66, 4) a.u. in Fig. 5(a). The rest of the charge density redistribution remains the same in both profile and magnitude.

The redistribution of charge density shown in Figs. 4–6 suggests that the interaction potential between the Li atom and graphene is composed of two distinct contributions: A screened Coulomb interaction resulting from the charge

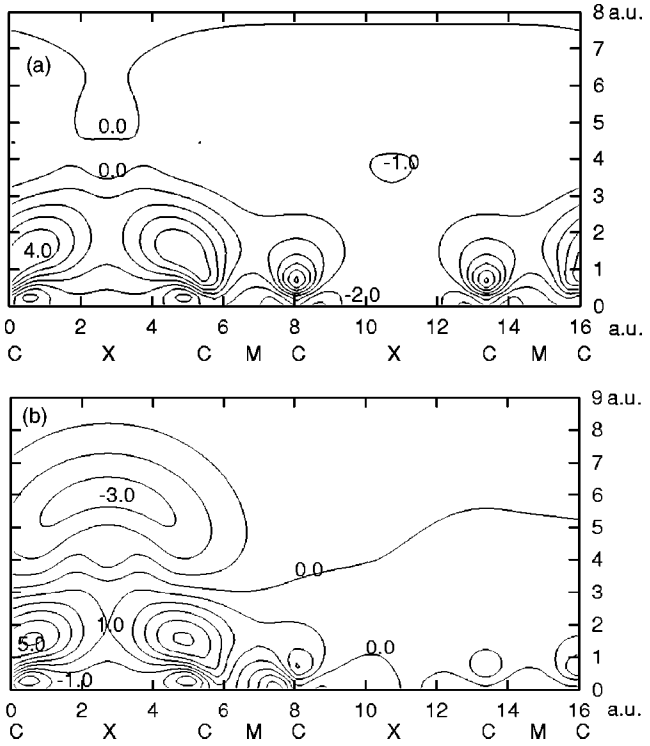

FIG. 6. The difference in charge density $\rho_{\mathrm{diff}}(\mathbf{r})$ on a plane perpendicular to graphene and containing the Li atom for configurations A (a) and B (b). The Li is positioned 4.0 a.u. above the graphene layer and its coordinates are (2.66, 4.0) a.u. The units of the electron density are $1.0\times10^{-3}e/(\mathrm{a.u.})^3$. The contours are equally spaced with an interval $1.0\times10^{-3}e/(\mathrm{a.u.})^3$. Contours closest to the graphene layer correspond to negative values and indicate net loss of electron density.

transfer between Li and C atoms and a van der Waals–type interaction. The interactions between carbon atoms in graphite can be written in the form of a 6-12 Lennard-Jones potential.[48] The system under consideration is a graphene layer and calculations show substantial changes in electron density at carbon nuclei for various positions of Li atom. We can therefore expect the van der Waals interaction to be somewhat different from the standard Lennard-Jones potential. It is possible to fit the interaction energy shown in Fig. 2 to the following analytical form:

$$U(x) = a_0 \frac{\exp(a_1 x)}{x} + \left\{ \frac{a_2}{x^4} + \frac{a_3}{x^6} + \frac{a_4}{x^{12}} \right\}. \qquad (2)$$

This fit is shown in Fig. 7 for configurations A and B and is valid when the Li position is greater than 1 a.u. above graphene. The above functional form is not adequate to describe the interaction potential of Li as it approaches the graphene plane (see Fig. 2). The fitted potential is, however, adequate for carrying out simulations on the Li-graphene system because of the high-energy barrier ($\sim$7 eV) as Li approaches the graphene layer. The first term in Eq. (2) represents the screened Coulomb potential of the Yukawa type. The terms in the curly bracket constitute a softer and longer-ranged inverse power-law potential. The fitting parameters are listed in Table II and correspond to interaction energies

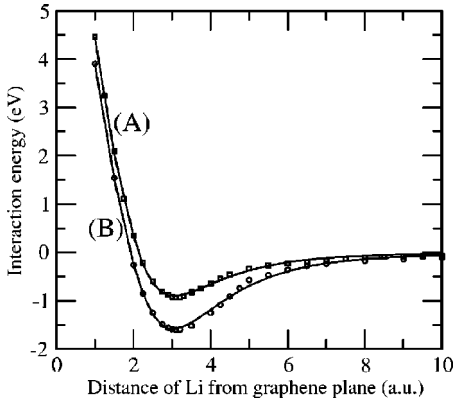

FIG. 7. The interaction potential of Li with graphene fitted to the function in Eq. (2) for Li positions in the range 1–10 a.u. Curves A and B denote configurations A and B, respectively. The symbols denote the calculated potential and the curve represents the fit using the values of the parameters in Table II.

expressed in eV and distance measured in a.u.

The cohesion between graphitic atoms when they are close together is described well by the LDA to the density functional theory. However, at large separations, this approach does not describe correctly the van der Waals interactions.[49–53] This is a consequence of treating the exchange and correlation within LDA which causes the dispersion energy to be underestimated at large separations of the atoms. A comparison of DFT-LDA calculation and multipole-polarization theory[54] shows that in purely graphitic structures, the accuracy of DFT-LDA calculations decreases rapidly for separations greater than 15% beyond the equilibrium value. A few methods[49,50,52] have been proposed to modify DFT-LDA methods in order to obtain the r^{-6} form for the van der Waals attraction at large separations. Based on previous studies for typical van der Waals systems[51,54] and, noting that the Li-graphene system is not a pure van der Waals system due to the significant charge redistribution, one can expect the DFT-LDA calculations to be inaccurate for separations substantially larger than the equilibrium position 3.1 a.u. in the Li-graphene system. Thus, the above fit to the potential may not be accurate for large distances. We are currently evaluating this correction to the DFT-LDA results. There is good evidence[51] that the DFT-LDA calculation reproduces well the repulsive part of the interaction resulting from the overlap of electrons on adjacent atoms even in systems where van der Waals forces are dominant. We do not expect any additional corrections in this region of the potential.

IV. SUMMARY

The energy of interaction between a Li atom and a graphene layer was computed for various positions of the Li

TABLE II. Fitted parameters for Li-graphene interaction potential (Fig. 2).

Configuration	a_0	a_1	a_2	a_3	a_4
A	562.586	−1.452	−289.287	192.685	−30.710
B	854.707	−1.360	−570.601	467.301	−112.15

atom using density functional theory. The energy of Li is lowest when it is at the center of the hexagonal ring formed by carbon at a distance of 3.1 a.u. from graphene. The equilibrium position of Li is not affected by the presence or absence of Li in next-nearest-neighbor hexagonal rings formed by carbon. The binding energy of Li is 1.598 eV when the separation between adjacent Li is 18.45 a.u. and the energy is 0.934 eV when the separation is 9.22 a.u. At the minimum energy configuration, there is a net gain of electron density in the region between the lithium atom and the carbon nuclei on planes parallel and perpendicular to graphene. Simultaneously, there is a net loss of electron density close to the graphene layer and around the lithium. This redistribution produces an optimum configuration of screened Coulomb interactions leading to a potential energy minimum. The equilibrium distance of Li above graphene is largely determined by the charge redistribution taking place in and around the hexagonal ring containing Li. This redistribution is not affected by interactions between Li atoms provided the separation is 9.22 a.u. or larger. The Coulomb repulsion between cations vanishes slowly as the distance of Li from the graphene layer increases to values greater than 10 a.u. The interaction potential of Li with graphene in configurations A and B can be fitted to a linear combination of screened Yukawa potential and a soft van der Waals potential represented by a sum of "4-6-12" inverse power-law functions.

ACKNOWLEDGMENTS

We gratefully acknowledge support of the National Science Foundation Grant No. 0100273 (NSF-EC Activity) which enabled this U.S.-Spain collaboration. The grant MCYT (MAT2002-04499) is also acknowledged for providing assistance.

[1] A. Herold, Bull. Soc. Chim. Fr. **187**, 999 (1955).
[2] R. Juza and V. Wehle, Naturwissenschaften **52**, 560 (1965).
[3] M. S. Dresselhaus and G. Dresselhaus, Adv. Phys. **30**, 1399 (1981).
[4] G. Pistolia, *Lithium Batteries: New Materials, Developments, and Perspectives* (Elsevier, New York, 1994).
[5] J. R. Dahn, T. Zheng, Y. H. Liu, and J. S. Xue, Science **270**, 590 (1995).
[6] J. E. Fischer, Chem. Innovation **30**, 21 (2000).
[7] M. S. Dresselhaus, G. Dresselhaus, and P. C. Eklund, *Science of Fullerenes and Carbon Nanotubes* (Academic, San Diego, 1996).
[8] R. Saito, G. Dresselhaus, and M. S. Dresselhaus, *Physical Properties of Carbon Nanotubes* (World Scientific, New York, 1998).
[9] P. Dubot and P. Cenedese, Phys. Rev. B **63**, 241402(R) (2001).
[10] C. Garau, A. Frontera, D. Quinonero, A. Costa, P. Ballester, and P. M. Deya, Chem. Phys. Lett. **374**, 548 (2003).
[11] E. C. Lee, Y. S. Kim, Y. G. Jin, and K. J. Chang, Phys. Rev. B **66**, 073415 (2002).
[12] Y. Liu, H. Yukawa, and M. Morinaga, Mol. Cryst. Liq. Cryst. **387**, 323 (2002).
[13] Y. Liu, H. Yukawa, and M. Morinaga, Adv. Quantum Chem. **42**, 315 (2003).
[14] V. Meunier, J. Kephart, C. Roland, and J. Bernholc, Phys. Rev. Lett. **88**, 075506 (2002).
[15] J. L. Yang, H. J. Liu, and C. T. Chan, Phys. Rev. B **64**, 085420 (2001).
[16] J. Zhao, A. Buldum, J. Han, and J. P. Lu, Phys. Rev. Lett. **85**, 1706 (2000).
[17] A. Claye and J. E. Fischer, Mol. Cryst. Liq. Cryst. **340**, 743 (2000).
[18] A. S. Claye, J. E. Fischer, C. B. Huffman, A. G. Rinzler, and R. E. Smalley, J. Electrochem. Soc. **147**, 2845 (2000).
[19] L. Duclaux, Carbon **40**, 1751 (2002).
[20] B. Gao, A. Kleinhammes, X. P. Tang, C. Bower, L. Fleming, Y. Wu, and O. Zhou, Chem. Phys. Lett. **307**, 153 (1999).
[21] G. Maurin, C. Bousquet, F. Henn, P. Bernier, R. Almairac, and B. Simon, Chem. Phys. Lett. **312**, 14 (1999).
[22] H. Shimoda, B. Gao, X. P. Tang, A. Kleinhammes, L. Fleming, Y. Wu, and O. Zhou, Phys. Rev. Lett. **88**, 015502 (2002).
[23] B. Gao, C. Bower, J. D. Lorentzen, L. Fleming, A. Kleinhammes, X. P. Tang, L. E. McNeil, Y. Wu, and O. Zhou, Chem. Phys. Lett. **327**, 69 (2000).
[24] H. Shimoda, B. Gao, X. P. Tang, A. Kleinhammes, L. Fleming, Y. Wu, and O. Zhou, Physica B **323**, 133 (2002).
[25] P. Chen, X. Wu, J. Lin, and K. L. Tan, Science **285**, 91 (1999).
[26] L. A. Girifalco, M. Hodak, and R. S. Lee, Phys. Rev. B **62**, 13 104 (2000).
[27] N. A. W. Holzwarth, S. Rabii, and L. A. Girifalco, Phys. Rev. B **18**, 5190 (1978).
[28] N. A. W. Holzwarth, L. A. Girifalco, and S. Rabii, Phys. Rev. B **18**, 5206 (1978).
[29] M. K. Song, S. D. Hong, and K. T. No, J. Electrochem. Soc. **148**, A1159 (2001).
[30] L. Bernasconi and P. A. Madden, J. Phys. Chem. B **106**, 12916 (2002).
[31] K. R. Kganyago and P. E. Ngoepe, Phys. Rev. B **68**, 205111 (2003).
[32] C. Jo, C. Kim, and Y. H. Lee, Phys. Rev. B **65**, 035420 (2002).
[33] M. Bockstedte, A. Kley, J. Neugebauer, and M. Scheffler, Comput. Phys. Commun. **107**, 187 (1997).
[34] M. Fuchs and M. Scheffler, Comput. Phys. Commun. **119**, 67 (1999).
[35] N. Troullier and J. L. Martins, Phys. Rev. B **43**, 1993 (1991).
[36] L. Kleinman and D. M. Bylander, Phys. Rev. Lett. **48**, 1425 (1982).
[37] J. P. Perdew and Y. Wang, Phys. Rev. B **45**, 13 224 (1992).
[38] J. C. Boettger and S. B. Trickey, Phys. Rev. B **32**, 3391 (1985).
[39] M. M. Dacorogna and M. L. Cohen, Phys. Rev. B **34**, 4996 (1986).
[40] J. H. Cho, S. H. Ihm, and M. H. Kang, Phys. Rev. B **47**, 14 020 (1993).
[41] P. Staikov, A. Kara, and T. S. Rahman, J. Phys.: Condens. Matter **9**, 2135 (1997).
[42] C. S. Barrett, Acta Crystallogr. **9**, 671 (1956).
[43] M. S. Anderson and C. A. Swenson, Phys. Rev. B **31**, 668

(1985).
[44] D. R. Hamann, Phys. Rev. B **40**, 2980 (1989).
[45] F. D. Murnaghan, Proc. Natl. Acad. Sci. U.S.A. **30**, 244 (1944).
[46] J. S. Arellano, L. M. Molina, A. Rubio, and J. A. Alonso, J. Chem. Phys. **112**, 8114 (2000).
[47] J. S. Arellano, L. M. Molina, M. J. Lopez, A. Rubio, and J. A. Alonso, in *Electronic Properties of Novel Materials - Molecular Nanostructures*, edited by H. Kuzmany (American Institute of Physics, New York, 2000), p. 376.
[48] L. A. Girifalco and R. A. Lad, J. Chem. Phys. **25**, 693 (1956).
[49] K. Rapcewicz and N. W. Ashcroft, Phys. Rev. B **44**, 4032 (1991).
[50] Y. Andersson, D. Langreth, and B. I. Lundqvist, Phys. Rev. Lett. **76**, 102 (1996).
[51] L. A. Girifalco and M. Hodak, Phys. Rev. B **65**, 125404 (2002).
[52] W. Kohn, Y. Meir, and D. E. Makarov, Phys. Rev. Lett. **80**, 4153 (1998).
[53] J. M. Perez-Jorda and A. D. Becke, Chem. Phys. Lett. **233**, 134 (1995).
[54] J. M. Pacheco and J. P. Ramalho, Phys. Rev. Lett. **79**, 3873 (1997).